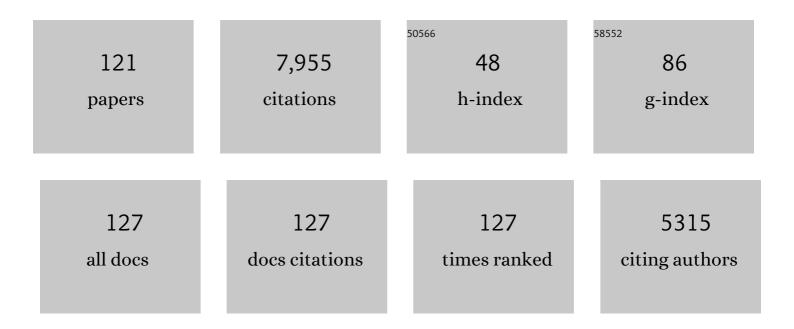
## W Steven Holbrook

List of Publications by Year in descending order

Source: https://exaly.com/author-pdf/7212462/publications.pdf Version: 2024-02-01



#	Article	IF	CITATIONS
1	What Do P-Wave Velocities Tell Us About the Critical Zone?. Frontiers in Water, 2022, 3, .	1.0	13
2	Geophysical imaging of the Yellowstone hydrothermal plumbing system. Nature, 2022, 603, 643-647.	13.7	13
3	Geostatistical Rock Physics Inversion for Predicting the Spatial Distribution of Porosity and Saturation in the Critical Zone. Mathematical Geosciences, 2022, 54, 1315-1345.	1.4	3
4	Limited Mantle Hydration by Bending Faults at the Middle America Trench. Journal of Geophysical Research: Solid Earth, 2021, 126, e2020JB020982.	1.4	18
5	The Effect of Aspect and Elevation on Critical Zone Architecture in the Reynolds Creek Critical Zone Observatory: A Seismic Refraction Study. Frontiers in Water, 2021, 3, .	1.0	6
6	Quantifying Depthâ€Ðependent Seismic Anisotropy in the Critical Zone Enhanced by Weathering of a Piedmont Schist. Journal of Geophysical Research F: Earth Surface, 2021, 126, e2021JF006289.	1.0	9
7	Resolving Deep Critical Zone Architecture in Complex Volcanic Terrain. Journal of Geophysical Research F: Earth Surface, 2020, 125, e2019JF005189.	1.0	13
8	Subsurface Weathering Revealed in Hillslopeâ€Integrated Porosity Distributions. Geophysical Research Letters, 2020, 47, e2020GL088322.	1.5	21
9	Crustal Structure of the Greenlandâ€iceland Ridge from Joint Refraction and Reflection Seismic Tomography. Journal of Geophysical Research: Solid Earth, 2020, 125, e2020JB019847.	1.4	15
10	Strong slopeâ€aspect control of regolith thickness by bedrock foliation. Earth Surface Processes and Landforms, 2020, 45, 2998-3010.	1.2	17
11	Porosity production in weathered rock: Where volumetric strain dominates over chemical mass loss. Science Advances, 2019, 5, eaao0834.	4.7	52
12	Characterizing the Critical Zone Using Borehole and Surface Nuclear Magnetic Resonance. Vadose Zone Journal, 2019, 18, 1-18.	1.3	19
13	Spatiotemporal Heterogeneity of Water Flowpaths Controls Dissolved Organic Carbon Sourcing in a Snow-Dominated, Headwater Catchment. Frontiers in Ecology and Evolution, 2019, 7, .	1.1	12
14	Links between physical and chemical weathering inferred from a 65-m-deep borehole through Earth's critical zone. Scientific Reports, 2019, 9, 4495.	1.6	72
15	Characterizing hydrological processes in a semiarid rangeland watershed: A hydrogeophysical approach. Hydrological Processes, 2019, 33, 759-774.	1.1	9
16	Seismic Characterization of Oceanic Water Masses, Water Mass Boundaries, and Mesoscale Eddies SE of New Zealand. Journal of Geophysical Research: Oceans, 2018, 123, 1519-1532.	1.0	10
17	Subsurface plantâ€accessible water in mountain ecosystems with a Mediterranean climate. Wiley Interdisciplinary Reviews: Water, 2018, 5, e1277.	2.8	90
18	Mapping Inherited Fractures in the Critical Zone Using Seismic Anisotropy From Circular Surveys. Geophysical Research Letters, 2018, 45, 3126-3135.	1.5	31

#	Article	IF	CITATIONS
19	Spatial delineation of riparian groundwater within alluvium deposit of mountainous region using Laplace equation. Hydrological Processes, 2018, 32, 30-38.	1.1	3
20	Reynolds Creek Experimental Watershed and Critical Zone Observatory. Vadose Zone Journal, 2018, 17, 1-20.	1.3	29
21	Estimating the water holding capacity of the critical zone using nearâ€surface geophysics. Hydrological Processes, 2018, 32, 3308-3326.	1.1	59
22	Critical Zone Structure Under a Granite Ridge Inferred From Drilling and Threeâ€Đimensional Seismic Refraction Data. Journal of Geophysical Research F: Earth Surface, 2018, 123, 1317-1343.	1.0	70
23	Geophysical Measurements to Determine the Hydrologic Partitioning of Snowmelt on a Snowâ€Dominated Subalpine Hillslope. Water Resources Research, 2018, 54, 3788-3808.	1.7	32
24	A model of threeâ€dimensional topographic stresses with implications for bedrock fractures, surface processes, and landscape evolution. Journal of Geophysical Research F: Earth Surface, 2017, 122, 823-846.	1.0	52
25	Joint prestack waveform inversion and acoustic reverse time migration. , 2017, , .		3
26	Seismic estimates of turbulent diffusivity and evidence of nonlinear internal wave forcing by geometric resonance in the S outh C hina S ea. Journal of Geophysical Research: Oceans, 2017, 122, 8063-8078.	1.0	12
27	Measuring snow water equivalent from common-offset GPR records through migration velocity analysis. Cryosphere, 2017, 11, 2997-3009.	1.5	24
28	Mapping turbulent diffusivity associated with oceanic internal lee waves offshore Costa Rica. Ocean Science, 2016, 12, 601-612.	1.3	18
29	Near-surface adjoint tomography based on the discontinuous Galerkin method. , 2016, , .		5
30	Estimating snow water equivalent over long mountain transects using snowmobile-mounted ground-penetrating radar. Geophysics, 2016, 81, WA183-WA193.	1.4	25
31	pSIN: A scalable, Parallel algorithm for Seismic INterferometry of large-N ambient-noise data. Computers and Geosciences, 2016, 93, 88-95.	2.0	13
32	Geophysical imaging of shallow degassing in a Yellowstone hydrothermal system. Geophysical Research Letters, 2016, 43, 12,027.	1.5	39
33	Alongâ€strike structure of the <scp>C</scp> osta <scp>R</scp> ican convergent margin from seismic a refraction/reflection survey: Evidence for underplating beneath the inner forearc. Geochemistry, Geophysics, Geosystems, 2016, 17, 501-520.	1.0	4
34	Continental crust generated in oceanic arcs. Nature Geoscience, 2015, 8, 321-327.	5.4	94
35	Geophysical imaging reveals topographic stress control of bedrock weathering. Science, 2015, 350, 534-538.	6.0	249
36	2-D ocean temperature and salinity images from pre-stack seismic waveform inversion methods: an example from the South China Sea. Geophysical Journal International, 2015, 202, 800-810.	1.0	21

#	Article	IF	CITATIONS
37	Multiscale geophysical imaging of the critical zone. Reviews of Geophysics, 2015, 53, 1-26.	9.0	192
38	Geophysical constraints on deep weathering and water storage potential in the Southern Sierra Critical Zone Observatory. Earth Surface Processes and Landforms, 2014, 39, 366-380.	1.2	177
39	Constraining hydrologic interpretations using near-surface geophysical methods. , 2014, , .		0
40	Crustal structure across the Costa Rican Volcanic Arc. Geochemistry, Geophysics, Geosystems, 2013, 14, 1087-1103.	1.0	20
41	Estimating Oceanic Turbulence Dissipation from Seismic Images. Journal of Atmospheric and Oceanic Technology, 2013, 30, 1767-1788.	0.5	43
42	Mapping Non-Local Turbulent Breakdown of Oceanic Lee Waves Offshore Costa Rica Through Seismic Oceanography. Proceedings of Meetings on Acoustics, 2013, , .	0.3	2
43	Middle Miocene to early Pliocene oblique extension in the southern Gulf of California. , 2012, 8, 752-770.		47
44	Farallon slab detachment and deformation of the Magdalena Shelf, southern Baja California. Geophysical Research Letters, 2012, 39, .	1.5	26
45	Cascadia fore arc seismic survey: Openâ€access data available. Eos, 2012, 93, 521-522.	0.1	16
46	Structure and serpentinization of the subducting Cocos plate offshore Nicaragua and Costa Rica. Geochemistry, Geophysics, Geosystems, 2011, 12, n/a-n/a.	1.0	114
47	Seismic reflection imaging of large-amplitude lee waves in the Caribbean Sea. Geophysical Research Letters, 2011, 38, n/a-n/a.	1.5	16
48	The tail of the Storegga Slide: insights from the geochemistry and sedimentology of the Norwegian Basin deposits. Sedimentology, 2010, 57, 1409-1429.	1.6	7
49	Seismic evidence for fluids in fault zones on top of the subducting Cocos Plate beneath Costa Rica. Geophysical Journal International, 2010, , .	1.0	5
50	Seismic imaging of a thermohaline staircase in the western tropical North Atlantic. Ocean Science, 2010, 6, 621-631.	1.3	38
51	First images and orientation of fine structure from a 3-D seismic oceanography data set. Ocean Science, 2010, 6, 431-439.	1.3	14
52	Prestack waveform inversion for the water olumn velocity structure―the present state and the road ahead. , 2010, , .		4
53	Seismic Reflection Methods for Study of the Water Column. , 2009, , 11-20.		2
54	Images of internal tides near the Norwegian continental slope. Geophysical Research Letters, 2009, 36,	1.5	28

#	Article	IF	CITATIONS
55	Sound speed requirements for optimal imaging of seismic oceanography data. Geophysical Research Letters, 2009, 36, .	1.5	28
56	Origin of pockmarks and chimney structures on the flanks of the Storegga Slide, offshore Norway. Geo-Marine Letters, 2008, 28, 43-51.	0.5	79
57	Full waveform inversion of reflection seismic data for ocean temperature profiles. Geophysical Research Letters, 2008, 35, .	1.5	46
58	Seismic structure of the southern Gulf of California from Los Cabos block to the East Pacific Rise. Journal of Geophysical Research, 2008, 113, .	3.3	17
59	Threeâ€dimensional seismic imaging of the Blake Ridge methane hydrate province: Evidence for large, concentrated zones of gas hydrate and morphologically driven advection. Journal of Geophysical Research, 2008, 113, .	3.3	41
60	Seismic signal penetration beneath postrift sills on the Newfoundland rifted margin. Geophysics, 2008, 73, B99-B107.	1.4	9
61	Assessing methane release from the colossal Storegga submarine landslide. Geophysical Research Letters, 2007, 34, .	1.5	30
62	Variation in styles of rifting in the Gulf of California. Nature, 2007, 448, 466-469.	13.7	259
63	Evidence for asymmetric nonvolcanic rifting and slow incipient oceanic accretion from seismic reflection data on the Newfoundland margin. Journal of Geophysical Research, 2006, 111, .	3.3	49
64	Seismic velocity structure of the rifted margin of the eastern Grand Banks of Newfoundland, Canada. Journal of Geophysical Research, 2006, 111, n/a-n/a.	3.3	93
65	Correction to "Evidence for asymmetric nonvolcanic rifting and slow incipient oceanic accretion from seismic reflection data on the Newfoundland margin― Journal of Geophysical Research, 2006, 111, n/a-n/a.	3.3	3
66	A deep seismic investigation of the Flemish Cap margin: implications for the origin of deep reflectivity and evidence for asymmetric break-up between Newfoundland and Iberia. Geophysical Journal International, 2006, 164, 501-515.	1.0	44
67	Crustal structure across the Grand Banks-Newfoundland Basin Continental Margin - I. Results from a seismic refraction profile. Geophysical Journal International, 2006, 167, 127-156.	1.0	95
68	Crustal structure across the Grand Banks-Newfoundland Basin Continental Margin - II. Results from a seismic reflection profile. Geophysical Journal International, 2006, 167, 157-170.	1.0	46
69	Slide structure and role of gas hydrate at the northern boundary of the Storegga Slide, offshore Norway. Marine Geology, 2006, 229, 179-186.	0.9	107
70	Coupled geophysical constraints on heat flow and fluid flux at a salt diapir. Geophysical Research Letters, 2005, 32, .	1.5	29
71	Crustal and upper mantle seismic structure of the Australian Plate, South Island, New Zealand. Tectonophysics, 2005, 395, 113-135.	0.9	27
72	Ocean internal wave spectra inferred from seismic reflection transects. Geophysical Research Letters, 2005, 32, .	1.5	109

#	Article	IF	CITATIONS
73	Temperature contrasts in the water column inferred from amplitude-versus-offset analysis of acoustic reflections. Geophysical Research Letters, 2005, 32, .	1.5	29
74	Continental breakup and the onset of ultraslow seafloor spreading off Flemish Cap on the Newfoundland rifted margin. Geology, 2004, 32, 93.	2.0	124
75	Critically pressured free-gas reservoirs below gas-hydrate provinces. Nature, 2004, 427, 142-144.	13.7	167
76	Inferring crustal structure in the Aleutian island arc from a sparse wide-angle seismic data set. Geochemistry, Geophysics, Geosystems, 2004, 5, .	1.0	85
77	Continental crust under compression: A seismic refraction study of South Island Geophysical Transect I, South Island, New Zealand. Journal of Geophysical Research, 2004, 109, .	3.3	73
78	Composition and structure of the central Aleutian island arc from arc-parallel wide-angle seismic data. Geochemistry, Geophysics, Geosystems, 2004, 5, n/a-n/a.	1.0	98
79	Seismic reflection imaging of water mass boundaries in the Norwegian Sea. Geophysical Research Letters, 2004, 31, .	1.5	101
80	Thermohaline Fine Structure in an Oceanographic Front from Seismic Reflection Profiling. Science, 2003, 301, 821-824.	6.0	239
81	Structure of the SE Greenland margin from seismic reflection and refraction data: Implications for nascent spreading center subsidence and asymmetric crustal accretion during North Atlantic opening. Journal of Geophysical Research, 2003, 108, .	3.3	146
82	Lithospheric structure across oblique continental collision in New Zealand from wide-anglePwave modeling. Journal of Geophysical Research, 2003, 108, .	3.3	81
83	Seismic anisotropy in gas-hydrate- and gas-bearing sediments on the Blake Ridge, from a walkaway vertical seismic profile. Geophysical Research Letters, 2003, 30, .	1.5	25
84	Crustal structure of the ocean-continent transition at Flemish Cap: Seismic refraction results. Journal of Geophysical Research, 2003, 108, .	3.3	145
85	Direct seismic detection of methane hydrate on the Blake Ridge. Geophysics, 2003, 68, 92-100.	1.4	92
86	Escape of methane gas through sediment waves in a large methane hydrate province. Geology, 2002, 30, 467.	2.0	58
87	Migration of methane gas through the hydrate stability zone in a low-flux hydrate province. Geology, 2002, 30, 327.	2.0	114
88	Crustal construction of a volcanic arc, wide-angle seismic results from the western Alaska Peninsula. Journal of Geophysical Research, 2002, 107, EPM 4-1.	3.3	59
89	Methods for resolving the origin of large igneous provinces from crustal seismology. Journal of Geophysical Research, 2002, 107, ECV 1-1-ECV 1-27.	3.3	113
90	Gravity anomalies and crustal structure at the southeast Greenland margin. Journal of Geophysical Research, 2001, 106, 8853-8870.	3.3	57

#	Article	IF	CITATIONS
91	Mantle thermal structure and active upwelling during continental breakup in the North Atlantic. Earth and Planetary Science Letters, 2001, 190, 251-266.	1.8	227
92	Hybrid shortest path and ray bending method for traveltime and raypath calculations. Geophysics, 2001, 66, 648-653.	1.4	48
93	Crustal structure of the southeast Greenland margin from joint refraction and reflection seismic tomography. Journal of Geophysical Research, 2000, 105, 21591-21614.	3.3	409
94	Structure and composition of the Aleutian island arc and implications for continental crustal growth. Geology, 1999, 27, 31.	2.0	277
95	Future of gas hydrate research. Eos, 1999, 80, 247-247.	0.1	6
96	Preliminary results from a geophysical study across a modern, continent-continent collisional plate boundary — the Southern Alps, New Zealand. Tectonophysics, 1998, 288, 221-235.	0.9	97
97	Natural gas hydrates on the southeast U.S. margin: Constraints from full waveform and travel time inversions of wide-angle seismic data. Journal of Geophysical Research, 1997, 102, 15345-15365.	3.3	106
98	U.S. mid-Atlantic margin structure and early thermal evolution. Journal of Geophysical Research, 1997, 102, 22855-22875.	3.3	39
99	Crustal structure of a transform plate boundary: San Francisco Bay and the central California continental margin. Journal of Geophysical Research, 1996, 101, 22311-22334.	3.3	62
100	Methane Hydrate and Free Gas on the Blake Ridge from Vertical Seismic Profiling. Science, 1996, 273, 1840-1843.	6.0	478
101	Underplating over hotspots. Nature, 1995, 373, 559-559.	13.7	13
102	Origin of thick, high-velocity igneous crust along the U.S. East Coast Margin. Journal of Geophysical Research, 1995, 100, 10077-10094.	3.3	187
103	The Edge Experiment and the U.S. East Coast Magnetic Anomaly. , 1995, , 155-181.		33
104	Deep structure of the U.S. Atlantic continental margin, offshore South Carolina, from coincident ocean bottom and multichannel seismic data. Journal of Geophysical Research, 1994, 99, 9155-9178.	3.3	122
105	Combined vertical-incidence and wide-angle seismic study of a gas hydrate zone, Blake Ridge. Journal of Geophysical Research, 1994, 99, 17975-17995.	3.3	86
106	Seismic structure of the U.S. Mid-Atlantic continental margin. Journal of Geophysical Research, 1994, 99, 17871-17891.	3.3	98
107	Crustal structure across the Brunswick magnetic anomaly, offshore Georgia, from coincident ocean bottom and multi-channel seismic data. Journal of Geophysical Research, 1994, 99, 21741-21757.	3.3	24
108	Seismic Evidence for a Lower-Crustal Detachment Beneath San Francisco Bay, California. Science, 1994, 265, 1436-1439.	6.0	74

#	Article	IF	CITATIONS
109	Large igneous province on the US Atlantic margin and implications for magmatism during continental breakup. Nature, 1993, 364, 433-436.	13.7	227
110	Deep seismic reflection data of EDGE U.S. mid-Atlantic continental-margin experiment: Implications for Appalachian sutures and Mesozoic rifting and magmatic underplating. Geology, 1993, 21, 563.	2.0	70
111	Image of the Moho across the continent-ocean transition, U.S. east coast. Geology, 1992, 20, 203.	2.0	27
112	Deep velocity structure of rifted continental crust, U.S. Midâ€Atlantic Margin, from wideâ€angle reflection/refraction data. Geophysical Research Letters, 1992, 19, 1699-1702.	1.5	19
113	Origins of deep crustal reflections: Implications of coincident seismic refraction and reflection data in Nevada. Geology, 1991, 19, 175.	2.0	36
114	The crustal structure of the Northwestern Basin and Range Province, Nevada, from wideâ€angle seismic data. Journal of Geophysical Research, 1990, 95, 21843-21869.	3.3	48
115	A petrological model of the laminated lower crust in Southwest Germany based on the wide-angle p- and s-wave seismic data. Geophysical Monograph Series, 1989, , 121-125.	0.1	2
116	An interpretation of wideâ€angle compressional and shear wave data in southwest Germany: Poisson's ratio and petrological implications. Journal of Geophysical Research, 1988, 93, 12081-12106.	3.3	111
117	The crustal structure of the axis of the Great Valley, California, from seismic refraction measurements. Tectonophysics, 1987, 140, 49-63.	0.9	47
118	A three-dimensional crustal model of southwest Germany derived from seismic refraction data. Tectonophysics, 1987, 142, 49-70.	0.9	63
119	Shearâ€wave velocity and Poisson's ratio structure of the upper lithosphere in southwest Germany. Geophysical Research Letters, 1987, 14, 231-234.	1.5	26
120	Seismic Studies of the Blake Ridge: Implications for Hydrate Distribution, Methane Expulsion, and Free Gas Dynamics. Geophysical Monograph Series, 0, , 235-256.	0.1	27
121	Probabilistic inference of subsurface heterogeneity and interface geometry using geophysical data. Geophysical Journal International, 0, , .	1.0	10